Available online at www.sciencedirect.com
ScienceDirect
International Journal of Heat and Fluid Flow 28 (2007) 299–305
International Journal of HEAT AND FLUID FLOW
www.elsevier.com/locate/ijhff

A note on the flow and heat transfer enhancement in a channel with built-in winglet pair

S.R. Hiravennavar [a], E.G. Tulapurkara [a,*], G. Biswas [b]

[a] Department of Aerospace Engineering, IIT Madras, Chennai 600036, India
[b] Department of Mechanical Engineering, IIT Kanpur, Kanpur 208016, India

Received 27 July 2005; received in revised form 8 December 2005; accepted 14 March 2006
Available online 30 June 2006

Abstract

Counter rotating longitudinal vortices produced by winglet in a channel are known to enhance heat transfer. In the present investigation the flow structure and heat-transfer enhancement by a winglet pair of non-zero thickness has been studied. A delta winglet pair type vortex generator is placed in a hydrodynamically developed and thermally developing laminar channel flow. Computations are done by solving the unsteady, three-dimensional, incompressible Navier–Strokes equations and energy equation using a modified Marker-and-Cell (MAC) method. The flow structure is complex and consists of main, corner and induced vortices. It is observed that as compared to a channel without winglets, the heat transfer is enhanced by 33% when single winglet is used and by 67% when a winglet pair is employed. Effects of thickness of the winglets and Reynolds number on the heat transfer augmentation are presented.

Keywords: Channel flow with vortex generator; Winglet pair; Heat transfer; Laminar flow

1. Introduction

Compact heat exchangers have wide applications in power, process, automotive and aerospace industries. Performance of these heat exchangers can be improved by adding protrusion type vortex generators such as fins, ribs, wings, winglets, etc. on the gas side of the core. When longitudinal vortex generators are placed near a heat transfer surface, they increase the heat transfer by transporting fluid from the wall into the free stream and vice versa. The effectiveness of a vortex generator in enhancing the heat transfer depends on the vortex strength generated per unit area of the vortex generator. A delta winglets pair kept at an angle of attack is very effective as the longitudinal vortices generated by it persist for hundreds of wing chords downstream of the winglets in the case of laminar channel flow (Fiebig et al., 1989). In the case of the heat exchangers the flow on gas side is usually laminar, because on this side the fin spacing is small and the mean velocity is low. With this application in mind, the delta winglet pair in a laminar flow is considered in the present investigation.

Edwards and Alker (1974) find that the delta winglets provided a higher overall heat transfer enhancement, compared to cubes placed on a flat plate. Experimental investigation of Katoaka et al. (1977) shows that the heat transfer is locally enhanced in the region where two neighboring vortices impose a flow toward the surface and the heat transfer locally decreases where the vortices impose a flow away from the surface. Fiebig et al. (1989) study the structure of velocity and temperature fields in laminar channel flows with wing-type longitudinal vortex generators and conclude that local enhancement of heat transfer coefficient increases by a factor of three compared to its value in a wingless channel. Fiebig et al. (1991) carry out an experimental comparison of delta wings, delta winglets, rectangular wings and rectangular winglets. Biswas and Chattopadhyay (1992) study heat transfer and skin friction characteristics in a channel with built-in wing-type vortex

* Corresponding author. Tel.: +91 44 22574000; fax: +91 44 22574002.
E-mail addresses: sadashiv_h@yahoo.co.in (S.R. Hiravennavar), egt@ae.iitm.ac.in (E.G. Tulapurkara), gtm@iitk.ac.in (G. Biswas).

0142-727X/$ - see front matter © 2006 Elsevier Inc. All rights reserved.
doi:10.1016/j.ijheatfluidflow.2006.03.030

generators at angle of attack (β) of 26° and Reynolds number of 500. They conclude that combined spanwise average Nusselt number shows increase of 34% even at the exit of a long channel. Deb et al. (1995) study heat transfer and flow structure in laminar and turbulent flows in a rectangular channel with longitudinal vortices. Biswas et al. (1996) carry out numerical and experimental study of flow structure and heat transfer effects of longitudinal vortices in a fully developed channel flow. They define a performance quality factor which indicates heat transfer enhancement for a given pressure loss penalty. Based on the value of this factor, they conclude that the performance of the winglet is best for β of 15°. Same trend is observed by Biswas et al. (1994), when the performance evaluation is done taking into account the energy transfer and the losses due to the thermodynamic irreversibilities. Sohankar and Davidson (2003) attempt unsteady three-dimensional Direct Numerical Simulation (DNS) and Large Eddy Simulation (LES) of heat and fluid flow in a plate-fin heat exchanger with thick rectangular winglet type vortex generators at Reynolds and Prandtl numbers of 2000 and 0.71, respectively. In the numerical investigations, except for the study of Sohankar and Davidson (2003), the winglet is idealized as of zero thickness. In the present study we consider winglet of finite thickness to render the computations more realistic.

2. Computational technique

The computation is performed in a channel, which is formed by two neighbouring fin-plates, with one pair of delta winglets placed inside it (Fig. 1). The solution is obtained by solving the three-dimensional, unsteady, Navier–Stokes equations and energy equation for an incompressible fluid. Hydrodynamically developed and thermally developing flow is considered.

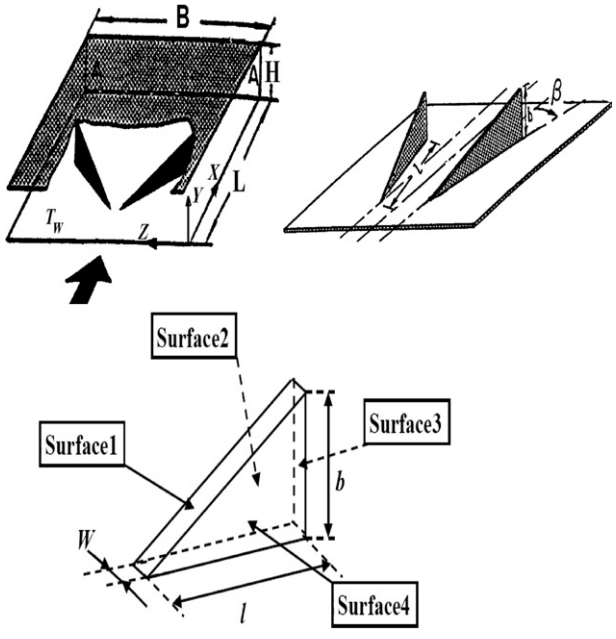

Fig. 1. Computational model and details of winglet geometry.

2.1. Governing equations

The equations for continuity, momentum and energy in non-dimensional form and standard tensor notation are

$$\frac{\partial u_i}{\partial x_i} = 0. \tag{1}$$

$$\frac{\partial u_i}{\partial \tau} + \frac{\partial (u_i u_j)}{\partial x_j} = -\frac{\partial p}{\partial x_i} + \frac{1}{Re}\left(\frac{\partial^2 u_i}{\partial x_j \partial x_j}\right). \tag{2}$$

$$\frac{\partial \theta}{\partial \tau} + \frac{\partial (u_i \theta)}{\partial x_i} = \frac{1}{Re \cdot Pr}\left(\frac{\partial^2 \theta}{\partial x_i \partial x_i}\right). \tag{3}$$

In the above equations, the velocity components are non-dimensionalised with the average velocity at the channel inlet (U_{avg}), all lengths with the channel height (H), and the pressure with ρU_{avg}^2. The non-dimensional temperature θ is defined as $\theta = \frac{T - T_\infty}{T_w - T_\infty}$ where T_w is wall temperature and T_∞ is entry temperature. Reynolds number, Re, in the above equations is defined as $Re = \frac{U_{avg} H}{\nu}$ where ν is the kinematic viscosity of the fluid. Air is used as working fluid.

2.2. Geometry

With reference to Fig. 1, The geometrical details of the flow simulation, are: (I) The height of the channel is H; the length of the channel (L) equals $11.4H$ and the aspect ratio of the channel ($\alpha = B/H$) equals 3, (II) The height of winglet (b) equals the channel height (H), the chord of the winglet (l) equals $2.46H$, the width of winglet (W) is a parameter ; the winglets are positioned such that their trailing edges are at $x = 2.856H$ from the inlet and the angle of attack (β) is 15°.

Though the geometry is symmetric the computation is done in the entire domain to capture unsteady flow features. Cartesian grid is used. The grid spacing in the three directions are $\Delta x/H$, $\Delta y/H$ and $\Delta z/H$. Their values depend on the grid size as well as the angle of the winglet and the channel aspect ratio. As the winglet surfaces are inclined to the coordinate directions, the grid is chosen such that the midpoint of grid element falls exactly on the winglet surface (See Hiravennavar, 2004 for details). A $98 \times 22 \times 97$ grid gives grid independent results.

2.3. Boundary conditions

The top and bottom surfaces are treated as no-slip walls and the side surfaces as free-slip boundaries. At the entrance to the channel a fully developed velocity profile is used and temperature is prescribed constant and equals T_∞. At the exit of the channel, the continuative boundary conditions are prescribed by setting second derivatives of the variables as zero. On the obstacle (winglet pair) no-slip boundary condition is specified for the velocities. The temperature of the winglet is constant and equals T_w.

2.4. Method of solution

The governing equations are solved by using modified Marker and Cell (MAC) method with staggered grid (see Biswas et al., 1996 for details). The velocity field is solved till a divergence free solution with an upper bound of 10^{-4} is obtained. After evaluating the correct velocity field, the energy equation is solved with a successive over relaxation (SOR) technique to determine the temperature field (see Biswas et al., 1996).

For the purpose of validation the computations are carried for channel with a single winglet at different angles of

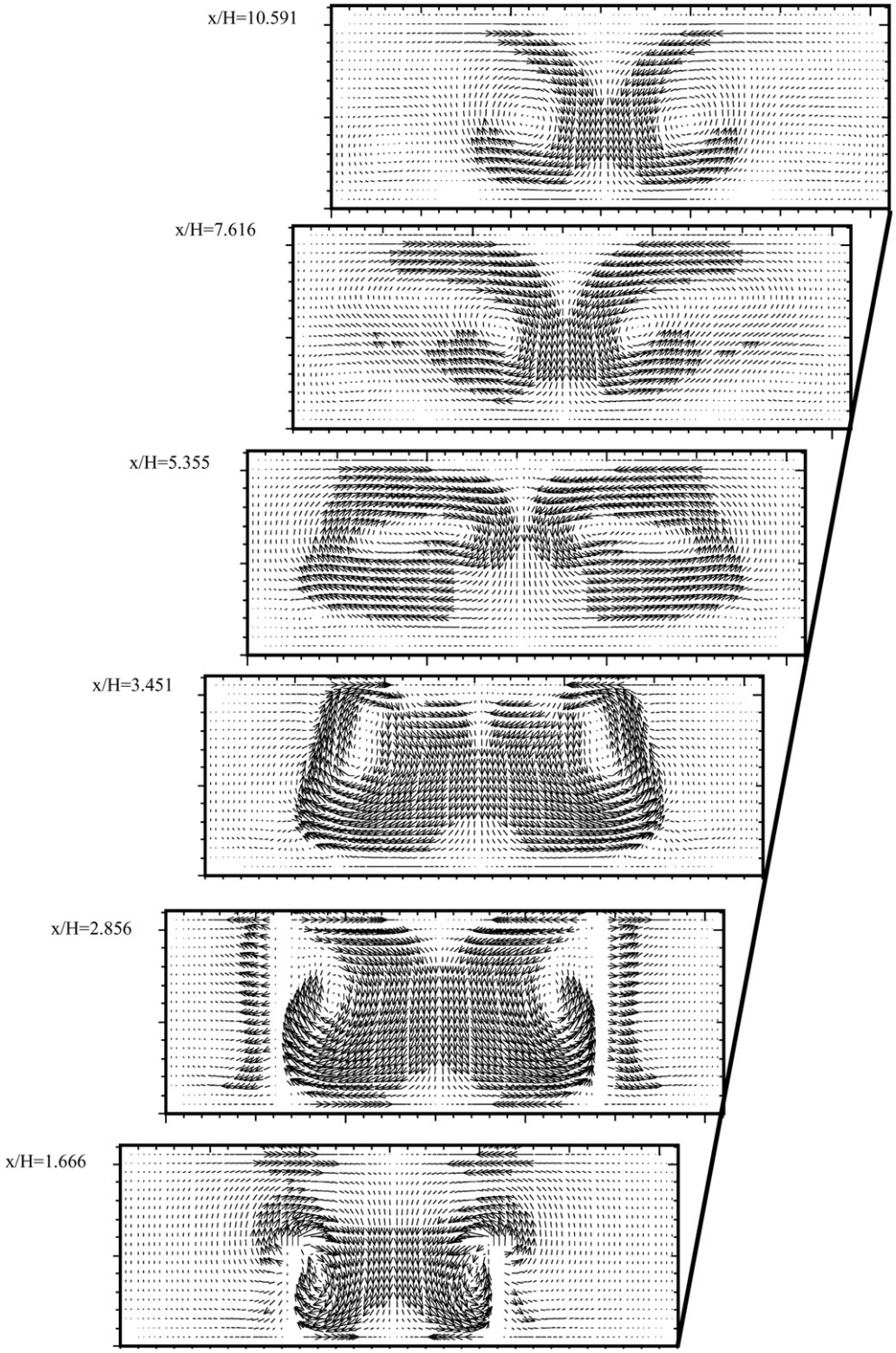

Fig. 2. Cross-stream velocity vectors at different locations along streamwise direction – $Re = 790$, $W/H = 0.0622$, $\alpha = 3$ and $\beta = 15°$.

attack. The computed results compare closely with experimental data of Biswas et al. (1996). Details can be found in Hiravennavar (2004).

Following Biswas et al. (1996) the computations are carried at $Re = 790$ and the winglet thickness (W) to height ratio (W/H) of 0.0622. Computations at other values of Re and W/H are also carried out.

3. Results and discussion

3.1. Flow structure

Development of the cross-flow velocity is shown in Fig. 2 for $Re = 790$. The plots show the generation of the vortices, their gradual deformation and decrease in their strength as they move downstream in the channel. The maximum cross-flow velocity at a plane is seen to be nearly equal to the mean axial velocity on that plane. The deformation of the vortical structure due to the channel walls can be seen when the cross-flow at any two stations downstream of the winglets are compared. Two counter-rotating main vortices behind the winglets cause the fluid to churn. This churning motion causes the fluid near the wall to flow in the central region and vice versa. It can be seen that the axes of main vortices move downward and away from each other as they (vortices) move downstream.

3.2. Heat transfer

The churning motion brings the hotter fluid at the walls to the mid region and increases the core temperature. At the same time it takes the cooler fluid from the mid region to the hot walls and increases the temperature gradients at the walls. The higher temperature gradients at the wall leads to higher heat transfer rates. In order to obtain a quantitative estimate of the heat transfer performance, the Nusselt number contours for the top and bottom plates

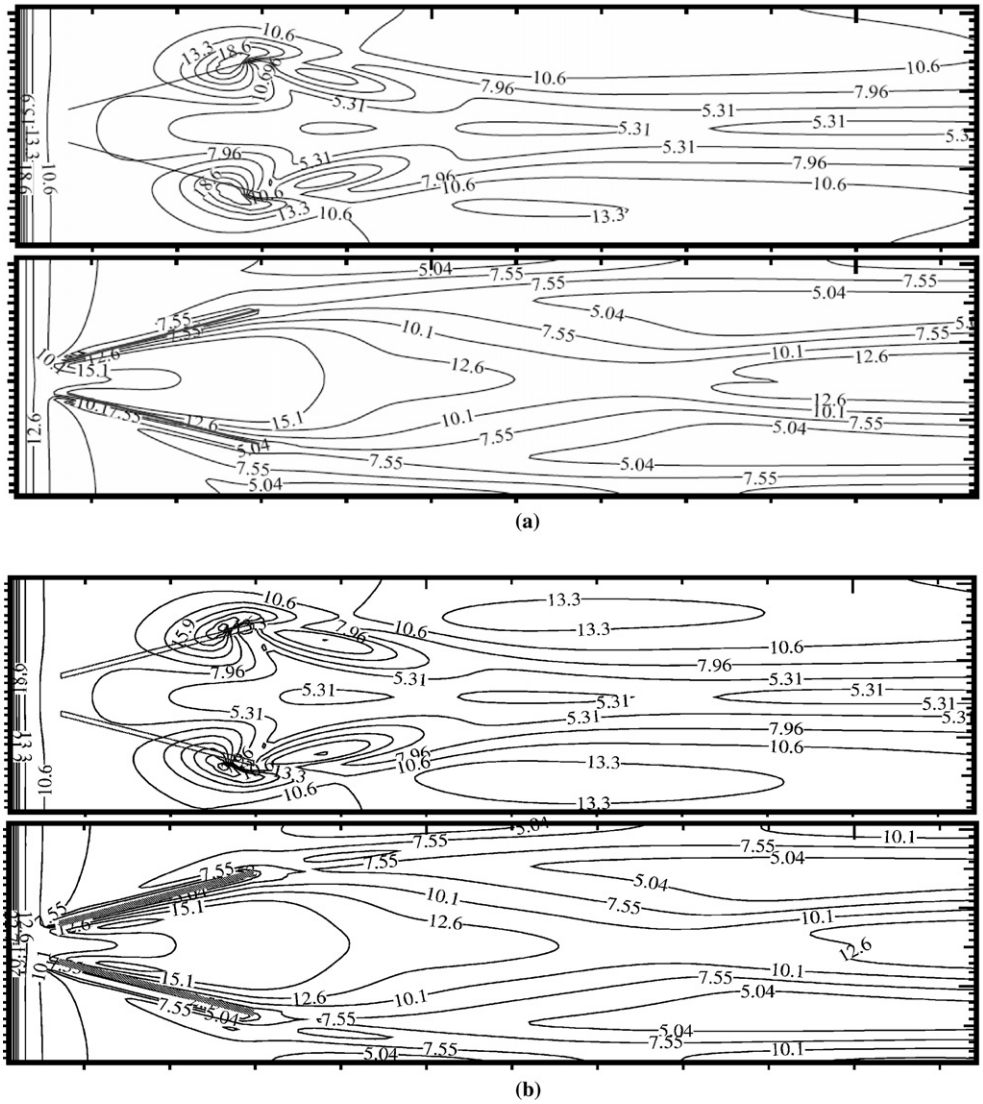

Fig. 3. Comparison of Nusselt number contours on top and bottom plates – $Re = 790$, $\beta = 15°$, and $\alpha = 3$. (a) Zero thickness winglet and (b) winglet with $W/H = 0.0622$.

are plotted. Nusselt number at a point (x, z) on plate is defined as $Nu = \frac{hH}{k} = -\frac{H\left(\frac{\partial T}{\partial y}\right)_w}{(T_w - T_b)}$ where T_b is the bulk temperature at a particular x location. Fig. 3 shows the contours of Nusselt number for winglet pairs of $W/H = 0$ and 0.0622. Fig. 3(a) shows that the heat transfer rate from bottom plate is more in the central portion as compared to that at the side array-symmetry walls. And for the top plate the heat transfer rate is lesser in the central portion as compared to that at the side array-symmetry walls. Fig. 3(b) shows that for winglet of finite thickness, $W/H = 0.0622$, the heat transfer rate is increased slightly at side array-symmetry walls and decreased slightly at central portion of the

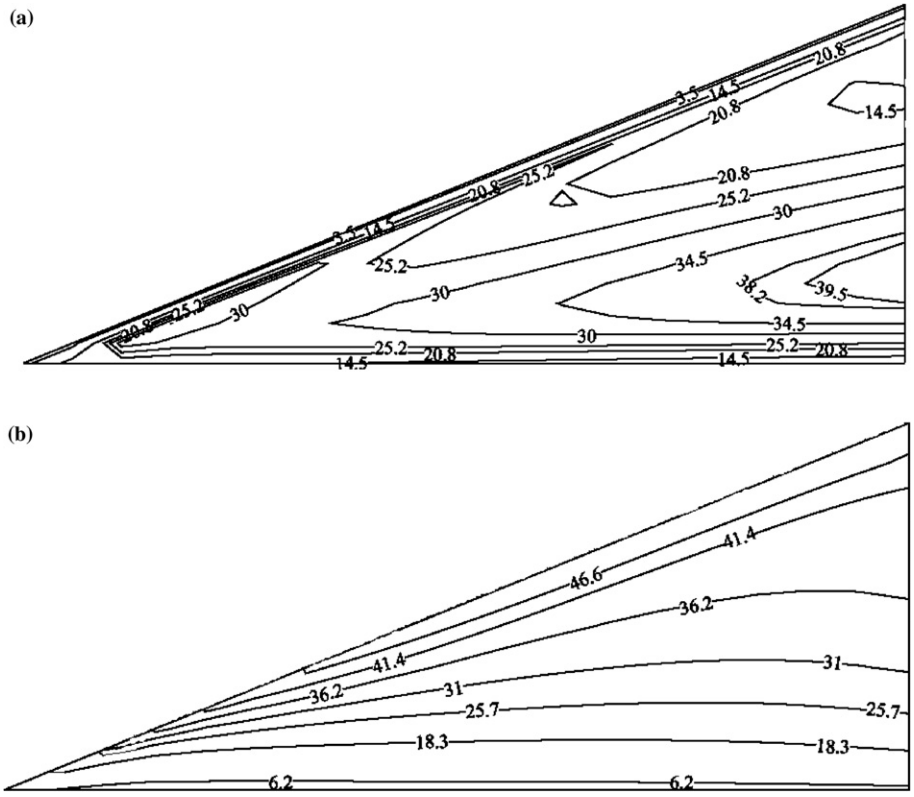

Fig. 4. Variation of Nusselt number over winglet surfaces – $Re = 790$, $\beta = 15°$, $\alpha = 3$ and $W/H = 0.0622$. (a) Surface facing center line and (b) surface facing walls.

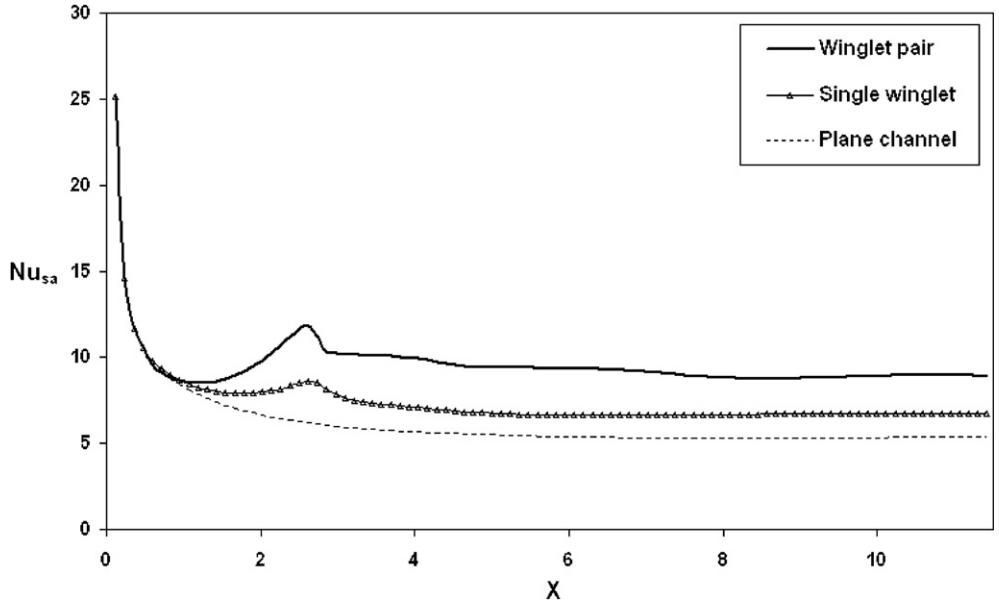

Fig. 5. Axial variation of average Nusselt number with and without winglet – $Re = 790$, $\beta = 15°$, $\alpha = 3$ and $W/H = 0.0622$.

channel for both top and bottom plates. Though heat transfer from top and bottom plates is of practical interest, the contours of Nusselt number on the surfaces of winglet are shown in Fig. 4 for the sake of completeness.

3.3. Effect of various parameters on heat transfer enhancement

We consider three types of parametric studies viz. (I) channel without winglet, with one winglet and a winglet pair, (II) variation of Reynolds number in case of winglet pair and (III) variation of the thickness of winglet for the case of winglet pair. For this study, we compare the values of spanwise average Nusselt number, $\overline{Nu}_{sa}$. It is defined as

$$\overline{Nu}_{sa} = \frac{B(q_1+q_2)(H/k)}{\int_0^B (T_{w1}(x,z)-T_b(x))\,dz + \int_0^B (T_{w2}(x,z)-T_b(x))\,dz}. \quad (4)$$

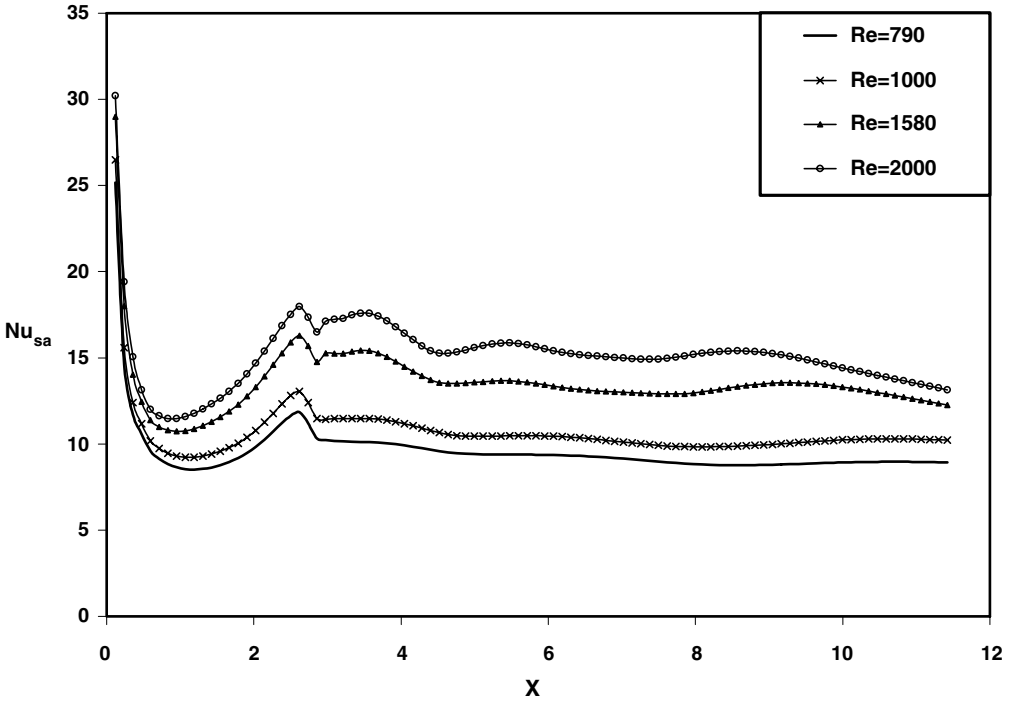

Fig. 6. Effect of Reynolds number on axial variation of average Nusselt number – $\beta = 15°$, $\alpha = 3$ and $W/H = 0.0622$.

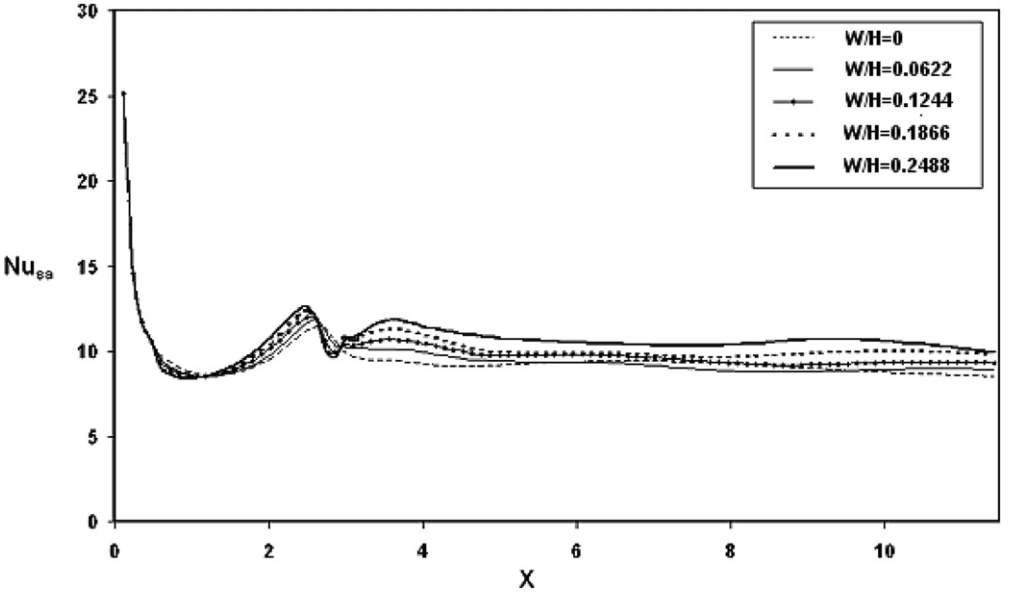

Fig. 7. Effect of thickness of the winglets on axial variation of average Nusselt number – $Re = 790$, $\beta = 15°$ and $\alpha = 3$.

Fig. 5 shows the axial variation of $\overline{Nu}_{sa}$ for the first parametric study viz. channel without winglet, with single winglet and with two winglets. The values of Re, α and W/H are 790, 3.0 and 0.0622, respectively. It is observed that $\overline{Nu}_{sa}$ is higher for the case with winglet pair as compared to single winglet case. At the end of the channel ($x/H = 11.42$) the winglet pair case shows as increase of 66.6% in Nusselt number as compared to the plane channel case and 33.1% as compared to the single winglet case. It is interesting to note that the enhancement in heat transfer due to a winglet pair is twice that of a single winglet.

To examine the effect of Reynolds number for the case with winglet pair, the computations are carried out at $Re = 790$, 1000, 1580, 2000. Fig. 6 shows the results for different Reynolds numbers. It is observed that as Re increases there is an increase in the heat transfer. At the end of the channel ($x/H = 11.42$), there is an increase of 37.6% when Re changes from 790 to 1580.

To study the influence of the thickness of winglet, the computations are carried out with $W/H = 0.0622$, 0.1244, 0.1866 and 0.2486. Fig. 7 shows the axial variation of $\overline{Nu}_{sa}$ in these cases. As thickness of the winglets increases, $\overline{Nu}_{sa}$ increases. As compared to the case of W/H of zero, the increase in the overall heat transfer of channel is 0.83%, 4.34%, 7.62% and 12.49% for $W/H = 0.0622$, 0.1244, 0.1866 and 0.2485, respectively. It is surmised that the finite thickness of winglet provides more cross sectional area for energy transfer from the bottom plate, and results in increased heat transfer.

4. Conclusions

A numerical simulation of laminar flow over a delta winglet pair in a channel has been performed at various Reynolds numbers and winglet thicknesses by solving the three-dimensional, unsteady, incompressible Navier–Stokes equations and the energy equation using modified MAC method. The enhancement in heat transfer due to a pair of winglets is almost twice that due to a single winglet. A winglet of finite thickness is marginally superior to the idealized zero thickness winglet.

Acknowledgements

The computations presented here are part of a project funded by Aeronautical Research and Development Board, India and are carried out at CFD Centre, IIT Madras started with funding from Department of Science and Technology, India. The support of funding agencies is gratefully acknowledged.

References

Biswas, G., Chattopadhyay, H., 1992. Heat transfer in a channel with built-in wing-type vortex generators. International Journal of Heat and Mass Transfer 35, 803–814.

Biswas, G., Deb, P., Biswas, S., 1994. Generation of longitudinal streamwise vortices – A device for improving heat exchanger design. Journal of Heat Transfer (ASME) 116, 588–597.

Biswas, G., Torii, K., Fujii, D., Nishino, K., 1996. Numerical and experimental determination of flow structure and heat transfer effects of longitudinal vortices in a channel flow. International Journal of Heat and Mass Transfer 39, 3441–3451.

Deb, P., Biswas, G., Mitra, N.K., 1995. Heat transfer and flow structure in laminar and turbulent flows in a rectangular channel in longitudinal vortices. International Journal of Heat and Mass Transfer 38, 2427–2444.

Edwards, F.J., Alker, G.J.R., 1974. The improvement of forced convection surface heat transfer using surface protrusions in the form of (a) cubes and (b) vortex generators. Proceedings of the Fifth International Heat Transfer Conference Tokyo 2, 2244–2248.

Fiebig, M., Brockmeier, U., Mitra, N.K., Guntermann, T., 1989. Structure of velocity and temperature fields in laminar channel flows with longitudinal vortex generators. Numerical Heat Transfer A-15, 281–302.

Fiebig, M., Kallweit, P., Mitra, N.K., Tiggelbeck, S., 1991. Heat transfer enhancement and drag by longitudinal vortex generators in channel flow. Experimental Thermal and Fluid Science 4, 103–114.

Hiravennavar, S.R., 2004. Numerical study of laminar flow and heat transfer in a channel with built-in winglet-pair type vortex generator, M.Tech. Thesis, Department of Aerospace Engineering, IIT Madras, May 2004.

Katoaka, K., Doi, H., Komai, T., 1977. Heat/mass transfer in Taylor vortex flow with constant axial flow rates. International Journal of Heat and Mass Transfer 20, 57–63.

Sohankar, A., Davidson, L., 2003. Numerical study of heat and fluid flow in a plate-fin heat exchanger with vortex generators. Turbulence Heat and Mass Transfer 4, 1155–1162.